

Article

An Improved CO₂ Separation and Purification System Based on Cryogenic Separation and Distillation Theory

Gang Xu, Feifei Liang, Yongping Yang *, Yue Hu, Kai Zhang and Wenyi Liu

Beijing Key Laboratory of Emission Surveillance and Control for Thermal Power Generation, School of Energy Power & Mechanical Engineering, North China Electric Power University, Beijing 102206, China; E-Mails: xgncepu@163.com (G.X.); liangffncepu@126.com (F.L.); hy8626566@163.com (Y.H.); kzhang@ncepu.edu.cn (K.Z.); lwy@ncepu.edu.cn (W.L.)

* Author to whom correspondence should be addressed; E-Mail: yypncepu@163.com; Tel.: +86-10-61772011.

Received: 4 March 2014; in revised form: 29 April 2014 / Accepted: 14 May 2014 /

Published: 23 May 2014

Abstract: In this study, an improved CO₂ separation and purification system is proposed based on in-depth analyses of cryogenic separation and distillation theory as well as the phase transition characteristics of gas mixtures containing CO₂. Multi-stage compression, refrigeration, and separation are adopted to separate the majority of the CO₂ from the gas mixture with relatively low energy penalty and high purity. Subsequently, the separated crude liquid CO₂ is distilled under high pressure and near ambient temperature conditions so that low energy penalty purification is achieved. Simulation results indicate that the specific energy consumption for CO₂ capture is only 0.425 MJ/kgCO₂ with 99.9% CO₂ purity for the product. Techno-economic analysis shows that the total plant investment is relatively low. Given its technical maturity and great potential in large-scale production, compared to conventional MEA and SelexolTM absorption methods, the cost of CO₂ capture of the proposed system is reduced by 57.2% and 45.9%, respectively. The result of this study can serve as a novel approach to recovering CO₂ from high CO₂ concentration gas mixtures.

Keywords: CO₂ recovery; cryogenic separation; conventional distillation; techno-economic analysis; oxy-fuel combustion

1. Introduction

One of the most sophisticated challenges in environmental protection in the 21st century is global warming, which is caused by large amounts of greenhouse gas emissions, especially CO₂. Measures must be taken to reduce CO₂ emissions and consequently restrain global warming. From the perspective of energy utilization, carbon capture and storage (CCS) is considered to be one of the most significant methods in CO₂ reduction [1], since it is reported that 90% of CO₂ emissions are generated by the combustion of fossil fuels, which will be extensively used in the foreseeable future [2].

Currently, several primary CO₂ capture and recovery methods are available: absorption (including chemical absorption and physical absorption), adsorption, membrane separation, and cryogenic separation [3–5]. Among these methods, chemical absorption can separate large amounts of high purity CO₂ from low concentration flue gas, but high energy penalty and huge investments are expected [5–7]. Physical absorption is an effective approach to recovering low purity CO₂ with low energy penalty, but additional energy is needed for sequent compression because the separated CO₂ is in the gas state [7–9]. Both absorption methods draw extensive attention because of their high technical maturity [5–9]. Adsorption and membrane separation are recognized as promising CO₂ capture methods despite inevitable problems such as low processing ability and high investment because of their operational feasibility and low separation energy penalty [10–16].

Cryogenic separation is a physical process that separates CO₂ under extremely low temperature. It enables direct production of liquid CO₂ at a low pressure, so that the liquid CO₂ can be stored or sequestered via liquid pumping instead of compression of gaseous CO₂ to a very high pressure, thereby saving on compression energy [17–20]. During the cryogenic separation process, the components of gas mixtures are separated by a series of compression, refrigeration, and separation steps. Since all these steps are highly mature technologies in the chemical industry, their operation and design feasibility can be guaranteed [20–22]. The cryogenic separation process requires no chemical agent, hence avoiding secondary pollution [17–22]. As far as industrial application is concerned, gas mixtures are usually composed of CO₂ and other gases, the boiling points of which are relatively low. These gases include H₂, N₂, O₂, Ar, and CH₄. These impurities lower the phase transition temperature of CO₂, which can even drop to under −80 °C. In this case, the refrigeration energy penalty increases substantially, and CO₂ frost formation becomes highly possible, thereby threatening equipment safety [23]. Attention should thus be paid to raising the phase transition temperature of CO₂ to improve the cryogenic separation method and consequently avoid facility freezing problems and high energy penalty [24–27].

Recently, many studies concerning cryogenic CO₂ separation methods have been conducted. For instance, Besong *et al.* [28] proposed a cryogenic liquefaction system whose mainstay is formed by compressor and flash unit, so the energy penalty decreases due to sufficient recovery of cold energy. Song *et al.* [29] developed a novel CO₂ capture process based on a Stirling cooler, whereby CO₂ is separated in liquid state after continuous cooling down by three Stirling coolers. Jana [30] researched the integration and optimization of a CO₂ capture system, and discussed the influences of several parameters on system performance. Based on the phase transition mechanism and the principle of energy cascade utilization, in a previous work we presented a novel system that simultaneously fulfills CO₂ separation and compression by adopting multi-stage compression and separation. Compared with conventional CO₂

capture methods, this novel system shows superior performance with $\text{CO}_2\text{-H}_2$ mixture and reduces the CO_2 recovery energy penalty by 65% and 15%, respectively [31].

Interestingly, the studies mentioned above mainly focus on achieving high CO_2 capture rates and low recovery energy penalties, whereas little attention is paid to the purity of the captured CO_2 . In fact, CO_2 purity in the product separated by the cryogenic separation method might be relatively low. For example, when applying the cryogenic separation method to separate CO_2 from $\text{CO}_2\text{-N}_2\text{-O}_2\text{-Ar}$ mixtures, the impurity content in the separated liquid can be as high as 2% to 5%; at this level, the CO_2 purity cannot satisfy the requirements of most industrial applications, as well as transport and storage [1,32,33].

In the present work, we propose an improved CO_2 separation and purification system that can separate the majority of the CO_2 in liquid state from the mixed gases with relatively low energy penalty via multi-stage compression, refrigeration, and separation. Furthermore, by introducing high pressure and near ambient temperature distillation into the improved system, CO_2 purity in the final product reaches 99.9%.

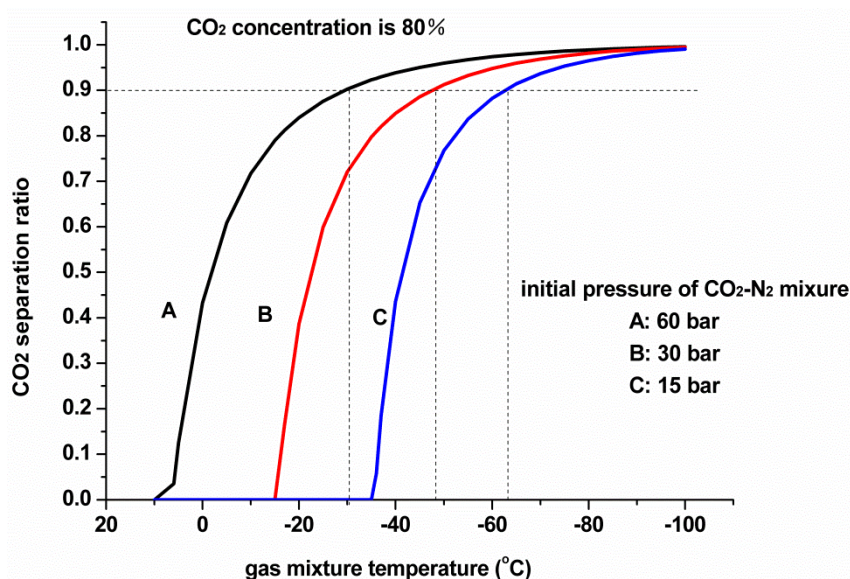
2. Proposal of the Cryogenic Separation Method

2.1. Phase Transition Characteristics of Mixed Gases Containing CO_2

In our previous works, the phase transition characteristics of $\text{CO}_2\text{-H}_2$ mixture (common in the syngas generated by shift reaction) were analyzed. Results indicate that CO_2 separation ratio is determined by two critical factors: the initial CO_2 concentration and the initial pressure of the gas mixture [31]. In the present study, we analyze the $\text{CO}_2\text{-N}_2\text{-O}_2\text{-Ar}$ mixture, which is common in oxy-fuel combustion.

Figure 1 presents the relationship between the CO_2 separation ratio and the temperature of $\text{CO}_2\text{-N}_2$ mixtures under different initial pressures, at an initial CO_2 concentration of 80%.

Figure 1. Variation in the initial pressure and CO_2 separation ratio of $\text{CO}_2\text{-N}_2$ with temperature.



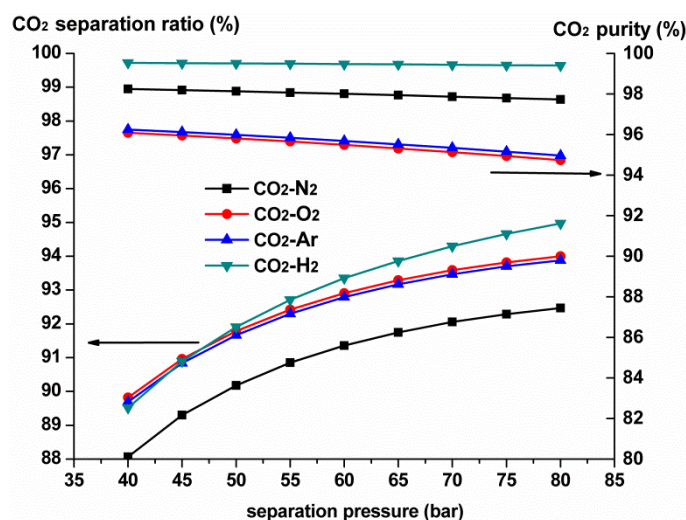
The CO_2 separation ratio increases as the initial pressure rises. Under the initial pressures of 15, 30, and 60 bar, to separate 90% CO_2 from the gas mixture, the temperature must be dropped to approximately $-63\text{ }^\circ\text{C}$, $-48\text{ }^\circ\text{C}$, and $-30\text{ }^\circ\text{C}$, respectively, so increasing the initial pressure is an

effective approach for improving the performance of the cryogenic separation method. Especially after the gas mixture enters the cryogenic CO₂ separation unit, the CO₂ concentration in the gas mixture continuously declines with CO₂ condensation. If the total pressure of the gas mixture could be increased at this moment, then CO₂ partial pressure will also increase, which is very important in maintaining the liquefaction temperature of CO₂ at a high level.

2.2. CO₂ Purity Characteristics of the Cryogenic Separation Method

Generally, a small amount of impurities always dissolve in the liquid CO₂ separated under high pressure, and the higher separation pressure, the larger the amount of impurities [28]. Figure 2 shows the variation in CO₂ purity and separation ratio under different separation pressures with four kinds of typical impurity compositions, at the initial CO₂ concentration of 80%. The following conclusions can be drawn based on Figure 2. On the one hand, the CO₂ separation ratio constantly increases with the increment of separation pressure, whereas the CO₂ purity in the product decreases. On the other hand, different impurity compositions have different effects on the CO₂ purity in the product. At the same separation pressure of 60 bar and initial CO₂ concentration of 80%, the CO₂ purity in the product of the CO₂-H₂ mixture is 99.47%, for the CO₂-N₂ mixture it's 98.01%, whereas for CO₂-O₂ and CO₂-Ar mixtures, it sharply reduces to 95.5% and 95.69%, respectively. This is because there exist significant differences in the physical properties of the different impurity gases, which affect the thermodynamic properties such as dew and bubble points, heat capacity, enthalpy and entropy of the CO₂ mixture, so the operating conditions and separation performance of the purification process will thus vary accordingly, resulting in different CO₂ purity in the product [27]. Generally, if the physical properties of the impurity gas are distinguished from those of the CO₂ (H₂ for example), it is easier to separate them by high pressure cryogenic separation [31]. However, for gas mixtures consisting of CO₂, N₂, O₂, and Ar, the CO₂ purity in the product attained by high pressure cryogenic separation is too low to satisfy the requirements of most industrial applications as well as transport and storage. Further purification measures should thus be considered.

Figure 2. Variation in CO₂ purity and separation ratio with different separation pressures and impurity compositions.

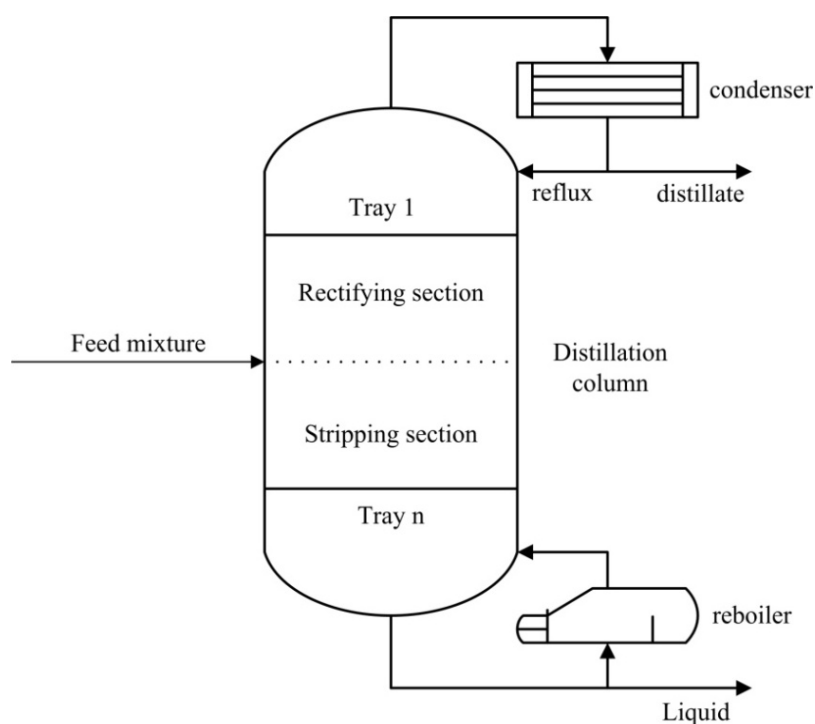


3. Distillation Mechanism and Feasibility Analysis

3.1. Distillation Mechanism

Distillation, which is the workhorse of chemical process industries, is widely used because of its high technical maturity [34,35]. It separates gas or liquid mixtures via consecutive partial vaporization and condensation in a distillation column. Figure 3 illustrates a simplified layout of the conventional distillation process. A feed mixture enters the column from the intermediate section. After condensing by the condenser installed on top of the column, part of the condensed liquid is refluxed, while the rest is discharged as distillate. Generally, the feed entrance divides the distillation column into two sections. The upper section is called the rectifying section, where the rising steam passes through the trays and comes in contact with the refluxed liquid to realize the material transfer and densification of volatile components [36]. Underneath the entrance is the stripping section, where the steam is heated by the reboiler located at the bottom of the column. Energy and material transfer proceeds as long as the heated steam is in countercurrent contact with the descending liquid, thus resulting in the accumulation of involatile components at the bottom.

Figure 3. Typical layout of the conventional distillation process.



3.2. Feasibility Analysis of Purifying CO₂ Mixture by Conventional Distillation

Certain conditions must be met when using conventional distillation to purify a mixture. In general, the basic condition lies in the difference in the boiling points of different components, the larger the difference, the easier to separate. In the meantime, operating pressure directly affects the performance of low temperature distillation. High pressure maintains the mixture completely in its critical state, thus lowering the possibility of separation. On the contrary, if the operating pressure is too low, then a large amount of refrigeration energy is required to maintain a low temperature at the top of the column.

Another fundamental condition of separating a mixture by conventional distillation is that it does not form azeotropes. In the temperature-composition diagram of an azeotrope, the vapor curve is tangent to the liquidus, this point of tangency is called the azeotropic point. Neither partial vaporization nor partial condensation can change the chemical composition of an azeotropic mixture at boiling point. That is, conventional distillation is not suitable for purifying azeotropic mixture near their boiling point.

Figures 4, 5, and 6 present the temperature-composition diagrams of $\text{CO}_2\text{-N}_2$, $\text{CO}_2\text{-O}_2$, and $\text{CO}_2\text{-Ar}$ mixtures, respectively. The following conclusions can be drawn based on the figures: (1) The differences in the boiling points of CO_2 and other impurities (*i.e.*, N_2 , O_2 , and Ar) are still very large, even under high pressure; (2) For $\text{CO}_2\text{-N}_2$, $\text{CO}_2\text{-O}_2$, and $\text{CO}_2\text{-Ar}$ mixtures, no azeotropic point is found under high pressure conditions, hence, purifying a CO_2 mixture consisting of impurities such as N_2 , O_2 , and Ar via conventional distillation is feasible. The distillation process can also be conducted under high pressure and near ambient temperature conditions, which ensures a low energy penalty.

Figure 4. Temperature-composition diagram of $\text{CO}_2\text{-N}_2$.

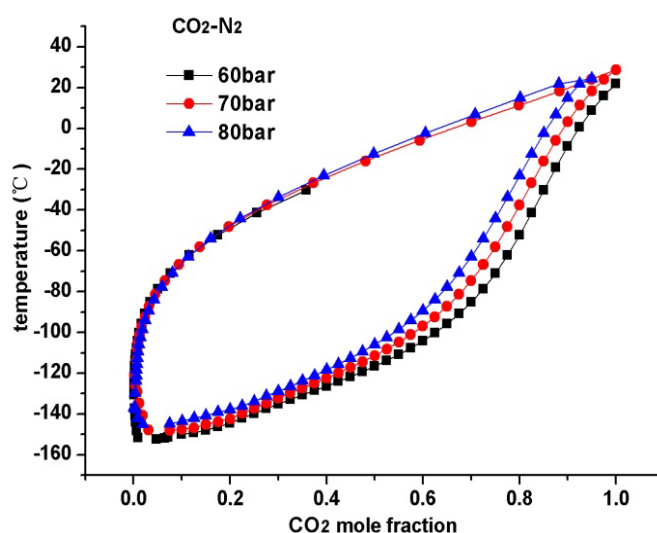


Figure 5. Temperature-composition diagram of $\text{CO}_2\text{-O}_2$.

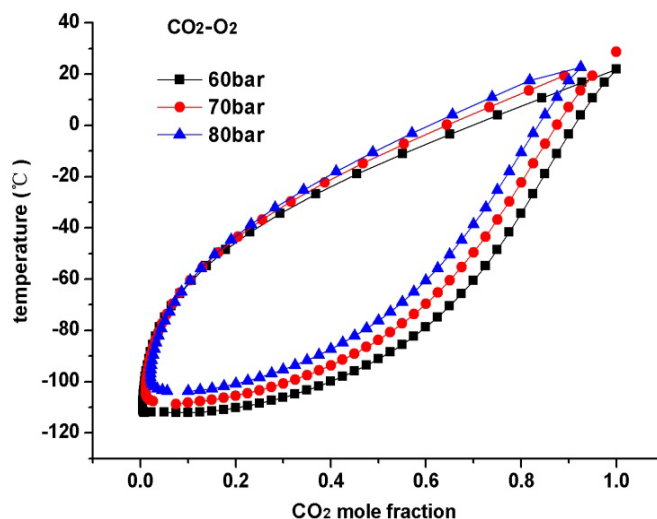
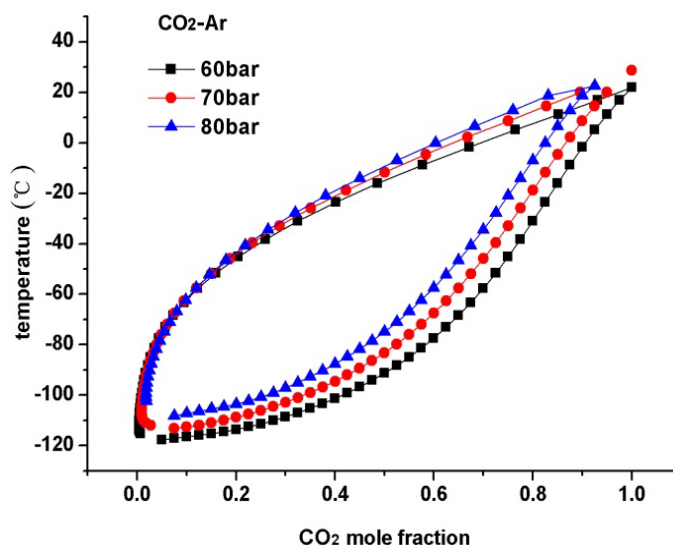


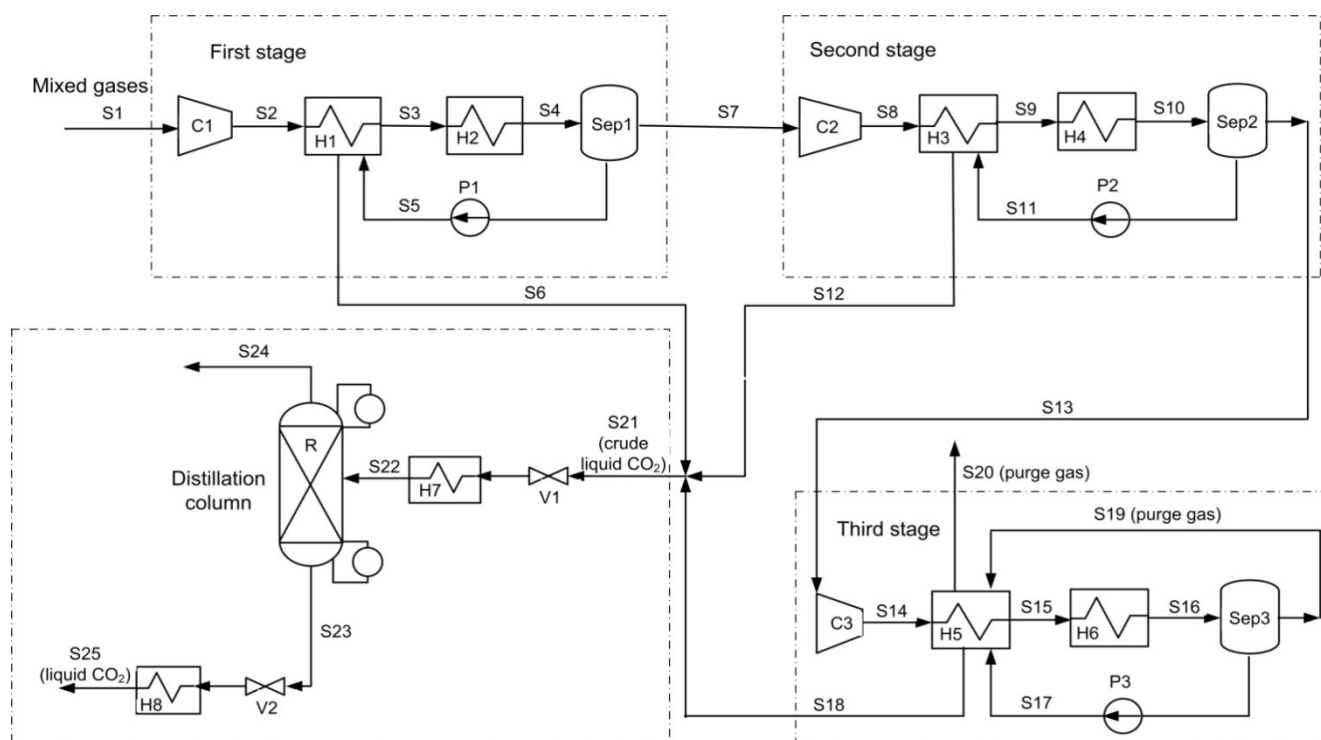
Figure 6. Temperature-composition diagram of CO₂-Ar.

4. Proposal and Performance Analysis of the Improved Separation and Purification System

4.1. Schematic Diagram of the Improved Separation and Purification System

Based on the analysis above, an improved CO₂ separation and purification system is proposed. The whole system is made up of two subsystems: the cryogenic separation subsystem and the distillation subsystem. According to the traditional cryogenic separation method, the liquefaction temperature increases by improving the initial pressure of the mixed gases. The separation ratio could also be maintained at a high level by multi-stage separation and compression. In the distillation subsystem, crude product is distilled under high pressure and near ambient temperature conditions. Figure 7 shows the schematic diagram of this improved system.

An initial dehydration of the mixed gases is performed before they are fed into the proposed system: by cooling down to near ambient temperature, the majority of H₂O is condensed and can be extracted out afterwards, while the rest is absorbed by a high-efficiency adsorbent (e.g., molecular sieve) [37]. As illustrated in Figure 7, when the dehydrated mixed gases (Stream 1 or S1) undergo the cryogenic separation and liquefaction processes, they are first compressed to an appropriate pressure (S2) by compressor 1 (C1). After cooling by the separation product, they would be cooled to a lower temperature by the external cold energy (S3). At this point, a part of the CO₂ is liquefied from the mixed gases. Using a gas-liquid separator (Sep1), we can separate the CO₂ from the mixture (S4) and pressurize it with a pump (P1). Then, part of the cold energy of the separated CO₂ (S5) is recovered back to the system by a heat exchanger (H1) with the mixed gases (S2) and leaves the system (S6). The abovementioned steps comprise the first stage of the process. If the mixed gases (S7) from the first stage could not satisfy the separation requirement, they are then separated in the second or the third stages. The processes of the next two stages are similar to the first one. In the cryogenic separation subsystem, three-stage separation and liquefaction are employed. When most of the CO₂ is separated, the purge gas (S20) leaves the system after its cold energy is recycled by a heat exchanger (H5).

Figure 7. Improved CO₂ separation and purification system.

The crude liquid CO₂ (S21) separated from the cryogenic separation subsystem is further purified in the distillation subsystem to improve its CO₂ purity. Before distillation, it is adjusted by a pressure regulating valve (V1) and a heat exchanger (H7). Temperatures on top and at the bottom of the distillation column (R) are precisely regulated within the range of $-20\text{ }^{\circ}\text{C}$ to $20\text{ }^{\circ}\text{C}$ and $-10\text{ }^{\circ}\text{C}$ to $30\text{ }^{\circ}\text{C}$, respectively. After adjustment by the pressure regulating valve (V2) and heat exchanger (H8), the CO₂ product with high purity (S25) is finally obtained. V1, V2, H7, and H8 can realize pressure and temperature adjustments to a small extent, thereby ensuring that the distillation process proceeds even in abnormal working conditions, such as start and stop. However, these adjustments are not necessarily needed in normal working conditions.

4.2. Simulations and Results Analysis

In this study, process simulation is conducted by ASPEN PLUSTM. The thermodynamic properties of the mixed gases are calculated by the PRMHV2 equations, because the prediction of the PRMHV2 equation can reflect the corresponding change trend of the mixture system when the initial parameters change, especially for nonpolar gas systems. The compressor and pump efficiencies are assumed to be 0.8, and the smallest temperature difference of the low-temperature heat exchanger is set at $2\text{ }^{\circ}\text{C}$.

Table 1 illustrates the main streams corresponding to Figure 7. As can be seen, after multi-stage compression, refrigeration, and separation, 92% of the CO₂ can be separated from the mixed gases in liquid state. The CO₂ concentrations of the crude liquid reaches 96.9%, at a pressure of 80 bar (S21). After distillation and adjustments in parameters, the CO₂ concentration in the final product is greatly improved to 99.9%, with the pressure decreasing to 60 bar (S23), which is suitable for most industrial applications as well as transport and storage.

Table 1. Parameters of the main points of the improved CO₂ separation and purification system.

Flow	Temperature (°C)	Pressure (bar)	Mass Flow (kg/s)	Mole Fraction (%)			
				CO ₂	N ₂	O ₂	Ar
S1	30.0	5	100.00	80.0	10.0	5.0	5.0
S2	30.0	21	100.00	80.0	10.0	5.0	5.0
S3	−26.5	21	100.00	80.0	10.0	5.0	5.0
S4	−35.0	21	100.00	80.0	10.0	5.0	5.0
S5	−29.7	80	62.93	98.5	0.4	0.5	0.6
S6	8.3	80	62.93	98.0	0.6	0.7	0.7
S7	−40.0	21	37.07	53.2	23.9	11.4	11.5
S8	10.4	38	37.07	53.2	23.9	11.4	11.5
S9	−25.0	38	37.07	53.2	23.9	11.4	11.5
S10	−40.0	38	37.07	53.2	23.9	11.4	11.5
S11	−31.0	80	13.35	93.8	2.1	2.1	2.0
S12	3.4	80	13.35	93.8	2.1	2.1	2.0
S13	−40.0	38	23.74	34.2	34.1	15.8	15.9
S14	−0.7	60	23.74	34.2	34.1	15.8	15.9
S15	−31.0	60	23.74	34.2	34.1	15.8	15.9
S16	−35.0	60	23.74	34.2	34.1	15.8	15.9
S17	−36.1	80	3.53	88.0	4.3	3.9	3.8
S18	−3.3	80	3.53	88.0	4.3	3.9	3.8
S19	−40.0	60	20.19	26.5	38.4	17.5	17.6
S20	−3.3	60	20.19	26.5	38.4	17.5	17.6
S21	7.3	80	79.81	96.9	1.1	1.1	1.0
S22	30.0	80	79.81	96.9	1.1	1.1	1.0
S23	22.5	60	76.18	99.9	9 ppm	48 ppm	27 ppm
S24	−10.8	60	3.62	40.5	20.1	20.0	19.3

The analysis data of the energy penalty for CO₂ recovery, along with some other performance parameters are summarized in Table 2. Note that the results and analysis of Table 2 are valid exclusively for the proposed system, which could be considered as polishing process instead of an intact CO₂ capture system, since the energy consumption of obtaining high CO₂ concentration is not taken into account here.

The proposed system clearly has excellent performance. The CO₂ recovery ratio is 90.04% with 99.9% CO₂ purity in the product, the energy penalty for the cryogenic separation subsystem is 29.77 MW, out of which C1, C2, and C3 consume 11.40, 2.21 and 0.72 MW, respectively; the total energy consumption for refrigeration is 18.34 MW (13.75, 3.41 and 1.18 MW for H2, H4 and H6); the total energy consumption for pumps is 0.519 MW (0.44, 0.07 and 0.009 MW for P1, P2 and P3, respectively), with 3.42 MW recovered by expansion; and the energy consumption of distillation is only 2.61 MW. In summary, the total energy penalty for this improved system is 32.38 MW, and the specific energy consumption for CO₂ capture is only 0.425 MJ/kgCO₂.

Table 2. Thermodynamic performance of the improved CO₂ separation and purification system.

Items	Value	Unit
Mass flux of mixed gases fed to the system	100	kg/s
Mole fraction of CO ₂ fed to the system	80	%
Mass flux of CO ₂ fed to the system	84.62	kg/s
Mass flux of captured CO ₂	76.18	kg/s
CO ₂ purity in product	99.9	%
CO ₂ recovery ratio	90.04	%
Energy penalty for cryogenic separation subsystem	29.77	MW
Energy consumption for distillation subsystem	2.61	MW
Total energy penalty for improved system	32.38	MW
Specific energy consumption for CO ₂ capture	0.425	MJ/kgCO ₂

The excellent performance of the proposed system can be attributed to its delicate process design, which is associated with highly mature technologies. The process and structural characteristics of the improved system are listed below:

- (1) Compression, refrigeration, and cryogenic separation are carried out several times in the system. Despite the fact that CO₂ concentration decreases continuously with CO₂ condensation, it can be improved by the increasing of the initial pressure, in order to maintain CO₂ liquefaction temperature at a high level. This condition in turn lowers the energy penalty for the cryogenic separation subsystem.
- (2) The distillation process is conducted under high pressure and near ambient temperature conditions. It can take full advantage of the large differences between the physical properties of the CO₂ and its impurities. It also connects perfectly with the cryogenic separation subsystem because the crude liquid CO₂ are under the same conditions. Consequently, the specific energy consumption for CO₂ capture could be as low as 0.425 MJ/kgCO₂.
- (3) As a result of the distillation process, the CO₂ purity in the product increases dramatically and finally meets the requirements for transport and storage. Note that higher CO₂ purity can be expected with simple parameter improvements, such as an increase in the number of distillation trays or an enhancement of the stripping rate. The final CO₂ product obtained by the proposed system then becomes available to special industries (e.g., food industry), thus enhancing its additional value.

5. Techno-Economic Analysis of the Proposed System

5.1. Component Overnight Cost Estimation

Given that our proposed system is similar to the cryogenic air separation unit (ASU), the reference data for component overnight cost estimation are gathered from the literature on ASU to ensure the calculation's accuracy and validity [38–41]. The calculation methodology employed to estimate the component overnight costs follows the method used by Holt and Kreutz in studies comparing alternative IGCC systems based on a series of EPRI-sponsored studies. The present work applies the overnight cost, which includes installation investment, balance of plant, general facilities costs, engineering fees, and contingencies [42,43]. Detailed reference data are listed in Table 3.

Table 3. Reference data for component overnight cost estimation.

Component	Scaling parameter	C_0 (M\$)	S_0	f	n^d	Notes
Compressor	Compression power	6.3	10 MWe	0.67	1	a
Heat exchanger	MAF coal input (LHV)	39.8	1377 MWth	0.67	1	a
Separator	Inlet flow rate	0.5	71250 ton/year	0.67	1	b
Distillation column	Inlet flow rate	0.12	17600 ton/year	0.67	1	c
Pump	Outlet pressure	0.093	80 bar	0.67	1	b

a: Costs taken from Agahi [38] and Lozza and Chiesa [39]; b: Gas-liquid separator is applied here; costs taken from El-Enin [40]; c: Data taken from Haas [41]; d: $n = 1$ for all components in the proposed system.

In general, the overnight component cost is the function of its own size. The overnight cost of a specific component can be obtained by the following equation:

$$C = nC_0 \left[\frac{S}{nS_0} \right]^f \quad (1)$$

where C_0 is the overnight cost of a single train reference component whose size is S_0 ; C is the overnight cost of a component whose size is S ; n is the number of equally sized trains operating at a capacity of $100\%/n$, and f is the scale factor.

5.2. Total Plant Investment

Total plant investment (TPI) is calculated as follows: TPI = total overnight cost (TOC) + interest during construction (IDC) [43]. According to Equation (1) and detailed parameters, overnight costs of major plant components are presented in Table 4. Notably, equipment made in China is generally much cheaper than that made in Western countries, essentially because of the low labor cost in China, as presented in literature [44–46].

Table 4. Summary of TPI calculation.

Overnight costs of plant components (M\$)	Value
C1	3.295
C2	1.767
C3	1.061
Heat Exchangers (H1–H8)	8.800
Sep1	3.747
Sep2	1.923
Sep3	1.425
Pumps (P1–P3)	0.279
Distillation Column (R)	3.825
Pipeline	2.500 ^e
Auxiliaries (<i>i.e.</i> , valves)	1.250 ^f
TOC	29.872
IDC	3.674
TPI	33.546
Annual O&M	1.342

e, f: Overnight costs for pipeline and auxiliaries are estimated to be approximately 8% and 4% of TOC, respectively.

The main economic analysis assumptions employed in this work are: (1) The lifespan of the proposed system is assumed to be 20 years with annual working hours set at 6000 h/year [47]; (2) IDC is taken as 12.3% of TOC based on a four-year construction schedule with equal annual payments and a real discount rate (k) of 10%/year; (3) The annual operation and maintenance cost (O&M) takes over 4% of TPI; (4) CO₂ transport and storage is charged for 5\$/ton, no extra carbon emission tax is attached.

The summary of the TPI calculation is shown in Table 4. TOC is 29.872 M\$ when major components and necessary auxiliaries such as pipelines and valves are considered. IDC is 3.674 M\$. The TPI of the proposed system is 33.546 M\$, and the annual O&M cost is 1.342 M\$.

Table 5 presents a brief performance comparison of several CO₂ recovery processes, including MEA absorption, SelexolTM absorption, and the proposed system. The techno-economic data of the MEA and SelexolTM absorption processes are collected from the IPCC report and related literature. The cost of CO₂ capture of the proposed system is calculated using the following equation:

$$\text{cost of CO}_2 \text{ capture} = \frac{[(\text{CRF})(\text{Total capture process investment})+(\text{Annual O\&M cost})+(\text{Annual cost on electricity})]}{\text{Annual CO}_2 \text{ captured}} \quad (2)$$

where the capital recovery factor (CRF) is related to the discounted rate (k) and the lifespan of the system (l); CRF is calculated as:

$$\text{CRF} = [k \cdot (1+k)^l] / [(1+k)^l - 1] \quad (3)$$

According to the previous calculation assumptions, CRF is equal to 0.117, whereas the total capture process investment and annual O&M cost are calculated based on Tables 2 to 5.

Table 5. Brief comparison of the techno-economic performance of several CO₂ recovery processes.

Items	Improved separation and purification system	MEA absorption process ^g	Selexol TM absorption process ^h
Mole fractions of flue gas			
CO ₂ (%)	80.00	13.30	29.14
N ₂ (%)	10.00	68.12	2.37
O ₂ (%)	5.00	3.81	0.00
Ar (%)	5.00	3.50	0.43
H ₂ O (%)	—	11.25	26.38
H ₂ (%)	—	—	40.13
Other (%)	—	0.02	1.55
Techno-economic indicators			
Mass flux of captured CO ₂ (kg/s)	76.18	113.33	66.83
CO ₂ recovery ratio (%)	90.04	90.0	87
CO ₂ purity in product (%)	99.9	98	95
Total energy penalty (MW)	32.38	441.9	62
Energy penalty for recovering unit CO ₂ (MJ/kgCO ₂)	0.425	3.9	0.928
Total capture process investment (M\$)	33.546	133.470	55.8
Specific capture process investment (M\$/(kg·s ⁻¹))	0.440	1.178	0.835
Cost of CO ₂ capture (\$/tCO ₂)	10.28	24	19

g: Data taken from Abu-Zahra [48] and the IPCC report (2007) [2]; h: Data taken from the IPCC report (2007) [2] and NETL (2002) [49].

As shown in Table 5, the specific capture process investment of the improved system is only $0.440 \text{ M}\$/(\text{kg}\cdot\text{s}^{-1})$, and its cost of CO_2 capture is $10.28 \text{ \$/tCO}_2$. As for the MEA and SelexolTM absorption methods, the specific capture process investments are $1.178 \text{ M}\$/(\text{kg}\cdot\text{s}^{-1})$ and $0.835 \text{ M}\$/(\text{kg}\cdot\text{s}^{-1})$, respectively, whereas their costs of CO_2 capture increase to $24 \text{ \$/tCO}_2$ and $19 \text{ \$/tCO}_2$, respectively. Which means compared to conventional MEA and SelexolTM absorption methods, the cost of CO_2 capture of the proposed system reduces by 57.2% and 45.9%, respectively.

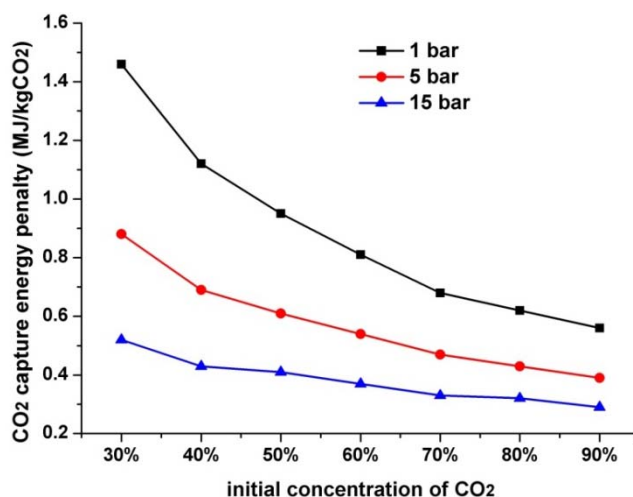
Note that the cost data found in related literature varies widely due to different estimation methods, design requirements, construction materials, and national conditions. Different recovery processes are applicable to various flue gas compositions, as revealed in Table 5. Hence, the improved system is not necessarily much better than or able to replace conventional absorption processes. We try to demonstrate in this study that if the initial CO_2 concentration of the gas mixture is relatively high (e.g., oxy-fuel combustion or pre-combustion capture), then the proposed system provides a feasible and competitive approach to CO_2 capture with respect to thermodynamic and economic performance. Briefly, performance of the proposed system in combination with oxy-fuel combustion is evaluated. The amount of oxygen needed for oxy-fuel combustion is roughly $65.4\text{--}75.7 \text{ kg/s}$ according to the law of conservation of mass, the energy consumption and additional investment of air separation unit are about $39\text{--}44 \text{ MW}$ and $39\text{--}42 \text{ M}\$$ with reference to related bibliography [44,50,51]. As a result, the total energy penalty for CO_2 capture will increase from 0.425 MJ/kgCO_2 to $0.937\text{--}1.003 \text{ MJ/kgCO}_2$, specific capture process investment will increase from $0.440 \text{ M}\$/(\text{kg}\cdot\text{s}^{-1})$ to $0.952\text{--}0.992 \text{ M}\$/(\text{kg}\cdot\text{s}^{-1})$, and cost of CO_2 capture will rise from $10.28 \text{ \$/tCO}_2$ to approximately $18.32\text{--}18.60 \text{ \$/tCO}_2$.

6. Discussion

6.1. Influences of Initial Pressure and Initial Concentration on the CO_2 Capture Energy Penalty

The initial pressure and initial concentration of the mixed gases have a great influence on the performance of the proposed system. Figure 8 presents the relationship between the CO_2 capture energy penalty against its initial pressure and concentration.

Figure 8. Relationship between CO_2 capture energy penalty against initial pressure and concentration.



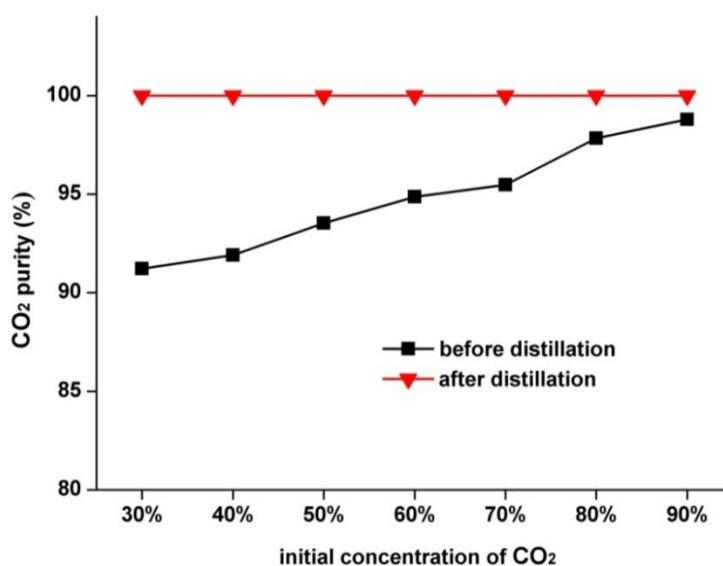
As shown in the curves, the energy penalty for CO₂ capturing unit greatly decreases with the increase in the initial pressure. In the proposed system, the mixed gases must first be compressed into a relatively high pressure to keep the liquefaction temperature at a high level, thus compression work of the first stage is relatively high and could consume over 30% to 50% of the total energy penalty. If the initial pressure of the mixed gases is relatively high at the beginning, lots of compression work could be saved for the first stage. The result is a decrease in the CO₂ capture energy penalty.

The CO₂ capture energy penalty also decreases substantially due to the increase of initial CO₂ concentration. As shown in Figure 8, the CO₂ capture energy penalty at an initial concentration of 60% increases by approximately 50% compared with that at an initial concentration of 80% in a fixed initial pressure. This value increases by approximately 150% when the initial concentration is 40%. This condition is due to in low initial CO₂ concentration, large refrigeration work is required to deal with the low liquefaction temperature. If the initial CO₂ concentration is enhanced, the CO₂ capture energy penalty will decrease significantly. In summary, the proposed system has superior performance in recovering CO₂ from mixed gases with high initial CO₂ concentration and initial pressure.

6.2. CO₂ Purity Comparison before and after Distillation

If the initial CO₂ concentration in the CO₂-N₂ mixture changes, the CO₂ purity in the final product obtained through the cryogenic separation method varies. Figure 9 provides the relationship between CO₂ purity and initial concentration of CO₂ before and after distillation. The CO₂ purity in the product is relatively low before distillation, although it is improved as the initial CO₂ concentration increases. Specifically, CO₂ purity without distillation is only 92% at an initial concentration of 30% and reaches only 98.78% at an initial CO₂ concentration of 90%. By contrast, the CO₂ purity in the product is constantly above 99.9% after distillation regardless of the initial CO₂ concentration. At this level, the CO₂ purity perfectly meets the requirements for most industrial applications as well as transport and storage. The distillation process can significantly improve the CO₂ purity in the product, thus proving that it is an effective and necessary purification method for separating CO₂-N₂ mixture.

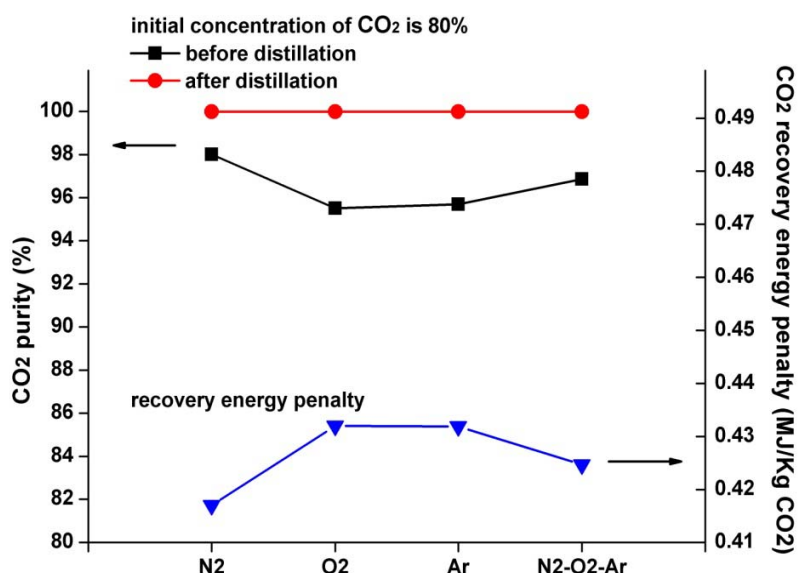
Figure 9. CO₂ purity comparison before and after distillation.



6.3. Analysis of the CO₂ Purity in the Product with Different Initial Compositions

Figure 10 shows the influences of different initial compositions on CO₂ purity and CO₂ recovery energy penalty. Supposing the initial CO₂ concentration of the mixed gases is 80%, four kinds of typical initial compositions are discussed: N₂, O₂, Ar, and N₂-O₂-Ar. The concentrations of these components are equally set at 20%. For N₂-O₂-Ar, the concentration of each component is 10%, 5%, and 5%, respectively. As can be seen, before distillation, the CO₂ purity is greatly affected by the change in initial composition. For N₂, O₂, Ar, and N₂-O₂-Ar, their CO₂ purities without distillation are only 98.01%, 95.5%, 95.69%, and 96.86%, respectively. After distillation, the CO₂ purity increases to more than 99.9% for all circumstances. The recovery energy penalty fluctuates within the range of 5% when the initial composition varies, which demonstrates that the proposed system presents excellent performance for various initial compositions.

Figure 10. Influences of different initial compositions on CO₂ purity and CO₂ recovery energy penalty.



7. Conclusions

Based on an in-depth analyses of cryogenic separation and distillation theory as well as the phase transition characteristics of gas mixtures containing CO₂, this study presents an improved CO₂ separation and purification system. According to the theoretical analysis, case simulations, and regularity analysis discussed above, the following conclusions are drawn:

- (1) By adopting multi-stage compression, refrigeration, and separation, the resulting improved cryogenic separation subsystem could separate the majority of CO₂ from gas mixtures with relatively low energy penalty and could fully recover the cold energy of the separation product.
- (2) Considering the large difference between the physical properties of CO₂ and other impurities, the distillation process is conducted under high pressure and near ambient temperature conditions. Consequently, the CO₂ purity in the product significantly increases to more than

99.9%, whereas the energy penalty for distillation is rather low. This condition finally realizes the low energy penalty of purification.

- (3) The cost of CO₂ capture of the proposed system is much lower than those of conventional absorption methods, because it mainly adopts common equipment which are widely utilized and highly mature in the chemical industry (e.g., compressors, heat exchangers, and pumps). Besides, this equipment can operate effectively for a long term under comparatively mild working condition as there is no serious corrosion or secondary pollution problems. Consequently, the TPI and annual O&M could be maintained at low levels.
- (4) The proposed system has superior performance in recovering CO₂ from mixed gases with high initial CO₂ concentration. Note that the high initial pressure of mixed gases contributes to lowering the CO₂ recovery energy penalty. Furthermore, the analysis proves that the proposed system can efficiently recover CO₂ from mixed gases, regardless of initial compositions as the CO₂ purity in the product could be as high as 99.9% under various circumstances.

Acknowledgments

This study was supported by the National Nature Science Fund of China (No. 51025624), National Key Technology R&D Program of China (2012BAC24B01), the 111 Project (B12034), and the Fundamental Research Funds for the Central Universities (2014ZD04).

Author Contributions

In this paper, Gang Xu provided the original idea and constructs its framework, and was responsible for drafting and revising the whole paper; Feifei Liang conducted the detailed calculation, simulation and contributes to revising the paper; Yongping Yang was the main technical guidance; Yue Hu devoted efforts to the writing of the techno-economic analysis in Section 5.1, and gave some valuable comments on revising the paper; Kai Zhang wrote the bulk of the distillation mechanism in Section 3.1; Wenyi Liu completed the further discussion of the proposed system in Section 6.2. All authors read and approved the manuscript.

Conflicts of Interest

The authors declare no conflict of interest.

References

1. Working Group III of the Intergovernmental Panel on Climate Change (IPCC). *IPCC Special Report on Carbon Dioxide Capture and Storage*; Cambridge University Press: Cambridge, UK, 2005.
2. Working Group III of the Intergovernmental Panel on Climate Change (IPCC). *IPCC's Fourth Assessment Report (AR4): Mitigation of Climate Change*; Cambridge University Press: Cambridge, UK, 2007.
3. Ma'mun, S.; Svendsen, H.F.; Hoff, K.A.; Juliussen, O. Selection of new absorbents for carbon dioxide capture. *Energy Convers. Manag.* **2007**, *48*, 251–258.

4. Saha, A.K.; Biswas, A.K.; Bandyopadhyay, S.S. Absorption of CO₂ in a sterically hindered amine: Modeling absorption in a mechanically agitated contactor. *Sep. Purif. Technol.* **1999**, *15*, 101–112.
5. Mandal, B.P.; Guha, M.; Biswas, A.K.; Bandyopadhyay, S.S. Removal of carbon dioxide by absorption in mixed amines: Modeling of absorption in aqueous MDEA/MEA and AMP/MEA solutions. *Chem. Eng. Sci.* **2001**, *56*, 6217–6224.
6. Alie, C.; Backham, L.; Croiset, E.; Douglas, P.L. Simulation of CO₂ capture using MEA scrubbing: A flowsheet decomposition method. *Energy Convers. Manag.* **2005**, *46*, 475–487.
7. Dorctor, R.D.; Molburg, J.C.; Thimmapuram, P.R. *Gasification Combined Cycle: Carbon Dioxide Recovery, Transport, and Disposal*; ANL/ESD-24; Argonne National Laboratory: Argonne, IL, USA, 1994.
8. Dorctor, R.D.; Molburg, J.C.; Thimmapuram, P.R. *KRW Oxygen-blown Gasification Combined Cycle: Carbon Dioxide Recovery, Transport, and Disposal*; ANL/ESD-34; Argonne National Laboratory: Argonne, IL, USA, 1996.
9. Zhang, J.; Webley, P.A.; Xiao, P. Effect of process parameters on power requirements of vacuum swing adsorption technology for CO₂ capture from flue gas. *Energy Convers. Manag.* **2008**, *49*, 346–356.
10. Na, B.K.; Koo, K.K.; Eum, H.M. CO₂ Recovery from flue gas by PSA process using activated carbon. *Korean J. Chem. Eng.* **2001**, *18*, 220–227.
11. Siriwardane, R.V.; Shen, M.S.; Fisher, E.P. Adsorption of CO₂ on molecular sieves and activated carbon. *Energy Fuels* **2001**, *15*, 279–284.
12. Siriwardane, R.V.; Shen, M.S.; Fisher, E.P. Adsorption of CO₂, N₂, and O₂ on natural zeolites. *Energy Fuels* **2003**, *17*, 571–576.
13. Gomes, V.G.; Yee, K.W.K. Pressure swing adsorption for carbon dioxide sequestration from exhaust gases. *Sep. Purif. Technol.* **2002**, *28*, 161–171.
14. Yan, S.P.; Fang, M.X.; Zhang, W.F.; Zhong, W.L.; Luo, Z.Y.; Cen, K.F. Comparative analysis of CO₂ separation from flue gas by membrane gas absorption technology and chemical absorption technology in China. *Energy Convers. Manag.* **2008**, *49*, 3188–3197.
15. Powell, C.E.; Qiao, G.G. Polymeric CO₂/N₂ gas separation membranes for the capture of carbon dioxide from power plant flue gases. *J. Membr. Sci.* **2006**, *279*, 1–49.
16. Feron, P.H.M.; Jansen, A.E. CO₂ separation with polyolefin membrane contactors and dedicated absorption liquids: Performances and prospects. *Sep. Purif. Technol.* **2002**, *27*, 231–242.
17. Pierce, W.F.; Riemer, P.; William, G.O. International perspectives and the results of carbon dioxide capture disposal and utilisation studies. *Energy Convers. Manag.* **1995**, *36*, 813–818.
18. Wang, B.Q. *Process Mechanism and System Synthesis for CO₂ Capture in IGCC System*; Chinese Academy of Sciences: Beijing, China, 2004.
19. Wang, B.Q.; Jin, H.G.; Han, W. IGCC system with integration of CO₂ recovery and the cryogenic energy in air separation unit. In Proceedings of ASME Turbo Expo, Vienna, Austria, 14–17 June 2004; GT-2004-53723.
20. Wang, B.Q.; Jin, H.G. A novel IGCC system with H₂/O₂ cycle and CO₂ recovery by ASU cryogenic energy. In Proceedings of the 7th International Conference on Greenhouse Gas Control Technologies, Vancouver, BC, Canada, 5–9 September 2004.

21. Deng, S.; Jin, H.; Cai, R. Novel cogeneration power system with LNG cryogenic exergy utilization. *Energy* **2004**, *29*, 497–512.
22. Zhang, N.; Lior, N. A novel near-zero CO₂ emission thermal cycle with LNG cryogenic exergy utilization. *Energy* **2006**, *31*, 1666–1679.
23. Song, C.F.; Kitamura, Y.; Li, S.H. Evaluation of Stirling cooler system for cryogenic CO₂ capture. *Appl. Energy* **2012**, *98*, 491–501.
24. Kanniche, M.; Gros-Bonnivarda, R.; Jauda, P.; Valle-Marcosa, J.; Amannb, J.M.; Boualloub, C. Pre-combustion, post-combustion and oxy-combustion in thermal power plant for CO₂ capture. *Appl. Therm. Eng.* **2010**, *30*, 53–62.
25. Zanganeh, K.E.; Shafeen, A. A novel process integration, optimization and design approach for large-scale implementation of oxy-fired coal power plants with CO₂ capture. *Greenh. Gas Control* **2007**, *1*, 47–54.
26. Zanganeh, K.E.; Shafeen, A.; Salvador, C. CO₂ capture and development of an advanced pilot-scale cryogenic separation and compression unit. *Energy Procedia* **2009**, *1*, 247–252.
27. Li, H.; Yan, J.; Yan, J.; Anheden, M. Impurity impacts on the purification process in oxy-fuel combustion based CO₂ capture and storage system. *Appl. Energy* **2009**, *86*, 220–213.
28. Besong, M.T.; Maroto-Valer, M.M.; Finn, A.J. Study of design parameters affecting the performance of CO₂ purification units in oxy-fuel combustion. *Int. J. Greenh. Gas Control* **2013**, *12*, 441–449.
29. Song, C.F.; Kitamura, Y.; Li, S.H.; Jiang, W.Z. Analysis of CO₂ frost formation properties in cryogenic capture process. *Int. J. Greenh. Gas Control* **2013**, *13*, 26–33.
30. Jana, A.K. Heat integrated distillation operation. *Appl. Energy* **2010**, *87*, 1477–1494.
31. Xu, G.; Li, L.; Yang, Y.P.; Tian, L.H.; Liu, T.; Zhang, K. A novel CO₂ cryogenic liquefaction and separation system. *Energy* **2012**, *42*, 522–529.
32. Xu, G.; Jin, H.G.; Yang, Y.P.; Duan, L.Q.; Han, W.; Gao, L. A novel coal-based hydrogen production system with low CO₂ emissions. *ASME J. Eng. Gas Turbines Power* **2010**, *132*, 031701–031709.
33. Xu, G.; Yang, Y.P.; Duan, L.Q.; Wang, N. A novel integration method for CO₂ separation and compression. *J. Eng. Thermophys.* **2010**, *31*, 1643–1646. (in Chinese)
34. Humphrey, J.L.; Siebert, A.F. Separation technologies: An opportunity for energy savings. *Chem. Eng. Prog.* **1992**, *88*, 80–92.
35. Engeliën, H.K.; Skogestad, S. Selecting appropriate control variables for a heat integrated distillation system with prefractionator. *Comput. Chem. Eng.* **2004**, *28*, 683–691.
36. Al-Muslim, H.; Dincer, I. Thermodynamic analysis of crude oil distillation systems. *Int. J. Energy Res.* **2005**, *29*, 637–655.
37. Toftegaard, M.B.; Brix, J.; Jensen P.A.; Glarborg, P.; Jensen, A.D. Oxy-fuel combustion of solid fuels. *Prog. Energy Combust. Sci.* **2010**, *36*, 581–625.
38. Agahi, R. *GE Power Systems*; Rotoflow, Inc.: Gardena, CA, USA, December 2002 personal communication.

39. Lozza, G.; Chiesa, P. CO₂ sequestration techniques for IGCC and natural gas power plants: A comparative estimation of their thermodynamic and economic performance. In Proceedings of International Conference on Clean Coal Technologies for our Future, Chia Laguna, Italy, 21–23 October 2002.
40. El-Enin, S.A.A.; Attia, N.K.; El-Ibiari, N.N.; El-Diwani, G.I.; El-Khatib, K.M. *In-situ* transesterification of rapeseed and cost indicators for biodiesel production. *Renew. Sustain. Energy Rev.* **2013**, *18*, 471–477.
41. Haas, M.J.; McAloon, A.J.; Yee, W.C.; Foglia, T.A. A process model to estimate biodiesel production costs. *Bioresour. Technol.* **2006**, *97*, 671–678.
42. Holt, N. IGCC Power Plants—EPRI Design and Cost Studies. In Proceedings of EPRI/GTC Gasification Technologies Conference, San Francisco, CA, USA, 6 October 1998.
43. Kreutz, T.; Williams, R.; Consonni, S.; Chiesa, P. Co-production of hydrogen, electricity and CO₂ from coal with commercially ready technology. Part B: Economic analysis. *Int. J. Hydrog. Energy* **2005**, *30*, 769–784.
44. Huang, B.; Xu, S.S.; Gao, S.H.; Liu, L.B.; Tao, J.Y.; Niu, H.W.; Cai, M.; Cheng, J. Industrial test and techno-economic analysis of CO₂ capture in Huaneng Beijing coal-fired power station. *Appl. Energy* **2010**, *87*, 3347–3354.
45. Zhao, M.; Minett, A.I.; Harris, A.T. A review of techno-economic models for the retrofitting of conventional pulverised-coal power plants for post-combustion capture (PCC) of CO₂. *Energy Environ. Sci.* **2013**, *6*, 25–40.
46. Huang, B.; Xu, S.S.; Gao, S.H.; Liu, L.B.; Tao, J.Y.; Niu, H.W.; Cai, M.; Cheng, J. Industrial test of CO₂ capture in Huaneng Beijing coal-fired power station. *Proc. CSEE* **2009**, *29*, 14–20. (In Chinese)
47. Nam, H.; Lee, T.; Lee, J.; Lee, J.; Chung, H. Design of carrier-based offshore CCS system: Plant location and fleet assignment. *Int. J. Greenh. Gas Control* **2013**, *12*, 220–230.
48. Abu-Zahra, M.R.M.; Niederer, J.P.M.; Feron, P.H.M.; Versteeg, G.F. CO₂ capture from power plants Part II. A parametric study of the economical performance based on mono-ethanolamine. *Int. J. Greenh. Gas Control* **2007**, *1*, 135–142.
49. Parsons, E.L.; Shelton, W.W.; Lyons, J.L. *Advanced Fossil Power Systems Comparison Study, Final Report Prepared for NETL*; National Energy Technology Laboratory: Morgantown, WV, USA, 2012.
50. Xiong, J.; Zhao, H.B.; Zheng, C.G.; Liu, Z.H.; Zeng, L.D.; Liu, H.; Qiu, J.R. An economic feasibility study of O₂/CO₂ recycle combustion technology based on existing coal-fired power plants in China. *Fuel* **2009**, *88*, 1135–1142.
51. Doukelis, A.; Vorrias, I.; Grammelis, P.; Kakaras, E.; Whitehouse, M.; Riley, G. Partial O₂-fired coal power plant with post-combustion CO₂ capture: A retrofitting option for CO₂ capture ready plants. *Fuel* **2009**, *88*, 2428–2436.